Cake Formation in 2-D Cross-Flow Filtration

Wei-Ming Lu and Kuo-Jen Hwang
Dept. of Chemical Engineering, National Taiwan University, Taipei, Taiwan, R.O.C.

The mechanism of cake formation is studied in 2-D cross-flow filtrations. By analyzing the forces exerted on a depositing particle, the value of the critical friction angle, β_c, which leads the particle to be stuck on the contact position, is determined. Not only the probability of particle deposition but also the size distribution of deposited particles can be calculated from the theoretical value of β_c. Numerical programs are constructed to simulate the packing structure and size distribution of particles in a formed cake and the path of cake compression. The local cake properties in the cake, such as local porosity and local specific filtration resistance, are also estimated by applying the design program and the data of filtration volume vs. time. The predicted values of average cake porosity and average specific filtration resistance agree very well with the experimental data.

Introduction

Cross-flow filtration is a mode of solid–liquid separation where slurry flows tangentially across the filter medium while filtrate permeates the septum vertically. Since the growth of cake will be limited by the shear stress acting on the surface of the filter medium, this mode of filtration has the advantages of thinner cake, higher filtration rate, and longer operating period compared to cake filtration. It has attracted not only the attention of plant engineers, but also many researchers in the field of filtration.

The attenuation of filtrate flux during a cross-flow filtration is always due to the deposition or fouling of particles, which form a so-called "dynamic membrane" on the primary membrane (Murkes and Carlsson, 1988). In order to understand the mechanism of formation of the dynamic membrane in the cross-flow filtration, several theories have been proposed. The concentration polarization theory has been used to predict the filtration rate at steady state by using a diffusion model (Porter, 1972; Zydney and Colton, 1986). This theory has been extended by Davis and Leighton (1987) to calculate the profiles of concentration and velocity of slurry in the polarized layer and by Romero and Davis (1988) to estimate the variation of the polarized layer thickness along the axial direction. Romero and Davis (1990) have developed a model to discuss the effects of operating parameters on the transient performance of cross-flow filtration. Applying the hydrodynamic model, various investigators (Green and Belfort, 1980; Kleinstreuer and Chin, 1984; Altena and Belfort, 1984; Belfort, 1989; Lu et al., 1993) have analyzed the flow pattern of fluid and trajectories of particles in a cross-flow filter. The transported flux of particles arriving at the filter medium is therefore given by the calculations. On the other hand, the phenomenon of selective deposition of particles in cross-flow filtration has been discussed by Fischer and Raasch (1986) and has been modified by Lu and Ju (1989) to derive a relationship among the physical properties of particles and operating conditions with the selective critical cut-diameter of deposited particles. In addition, the effects of the profiles of fluid velocity and particle concentration on the rate of particle deposition and the attenuation of filtration rate have been discussed by Lu et al. (1993). Although many researchers have studied the effects of operating variables on the performance of cross-flow filtration, none has focused attention on the properties of the formed cake that have very important influence on the rate of filtration.

Computer simulation has been widely used to study the packing structure of particles. Houi and Lenormand (1986) used a sticking model to describe the depositing process of spherical particles on filter fibers. The cake structure can be simulated under various sticking angles and various Peclet numbers of particles. Tassopoulos et al. (1990) have developed a discrete stochastic model to simulate the phenomena of particle deposition on a substrate surface. In their study, a probability concept was applied to take the Brownian motion of particles into account. Schmitz et al. (1990) have analyzed the flow pattern of a fluid near to and in the membrane pores

Correspondence concerning this article should be addressed to W.-M. Lu.

in a cross-flow filtration and have developed a trajectory model to simulate the particle deposition on the membrane surface. The phenomenon of cake compression during filtration, however, has not been considered. Sharma and Lei (1991) have studied the properties of a clay filter cake by using a structural network model, and the factors that affect the properties of filter cake have been also discussed. Lu and Hwang (1993) have studied the mechanism of cake formation in constant pressure "dead-end" cake filtrations. In their investigation, the concept of a critical friction angle between spherical particles was adopted to simulate the structure of the deposited filter cake. By considering the compression effect caused by liquid drag, they were able to predict the profiles of local cake properties, such as porosity, specific filtration resistance, and hydraulic pressure from a set of simple filtration data.

To study the mechanism of cake formation in cross-flow filtrations, this study analyzes the forces exerted on the depositing particle to find out how the particles will deposit on the cake surface. A numerical program is then designed to simulate the local cake properties, such as particle-size distribution, porosity, and specific filtration resistance, under various operating conditions.

Theory

Critical friction angle of particles on the cake surface

Particles in slurry are carried by liquid toward the filter septum and will deposit on the septum to form a filter cake during cross-flow filtration. Figure 1 depicts the formation of a filter cake in a cross-flow filtration system, in which particle B is a deposited particle while particle A is a particle just arriving at the surface of particle B. The angle of friction, β, shown in Figure 1 is introduced to examine the stability of particle A at the touching position. Since a larger value of β will result in less friction between these two particles, it will cause particle A to be more easily swept away from the contact point by the tangential bulk flow of slurry. When angle β is smaller than a critical value, β_c, there exists sufficient friction that causes particle A to deposit stably on particle B at the contact point. The schema of this selective deposition of particles is shown in Figure 2.

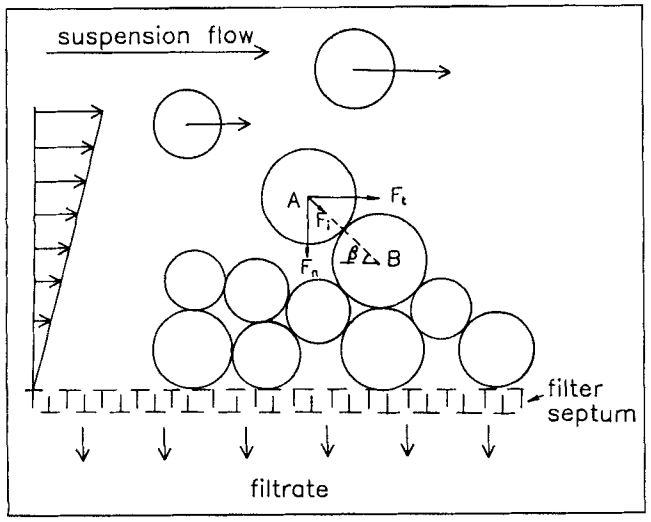

Figure 1. Forces exerted on the two characteristic particles staying on cake surface in a cross-flow filtration.

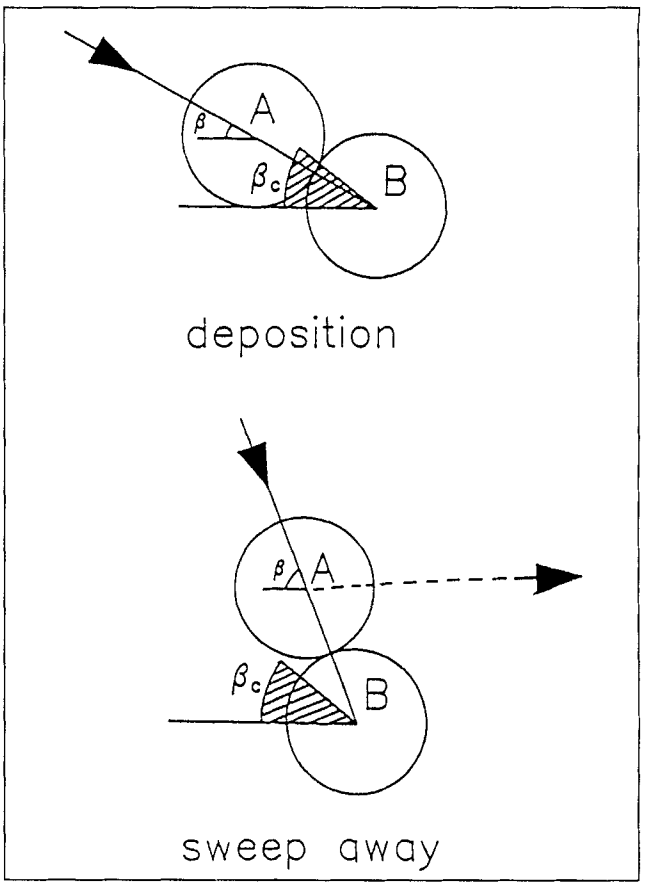

Figure 2. Selective deposition of particle *A* on particle *B*.

The value of critical angle of friction changes depending on the properties of particles, such as the interparticle forces, the shape and size distribution of particles, and the conditions of cross-flow filtration. Prior to obtaining the value of β_c in a cross-flow filtration for a given particle, the forces exerted on the depositing particles will be analyzed as follows.

Since the size of particles in a slurry is very small compared with the thickness of the laminar sublayer in a turbulent cross-flow filtration, the analysis of forces exerted on particle A is limited to that within the laminar sublayer. The drags and other forces exerted on particle A as shown in Figure 1 can be summarized as (1) tangential drag parallel to the filter medium, F_t; (2) net drag normal to the filter medium, F_n; (3) the net gravity force, F_g; and (4) interparticle forces, F_i (such as Van der Waals' force, electrostatic force). In the scope of this study, the diameter of most particles is limited to be larger than 1 μm, which makes the effect of Brownian motion of particles negligibly small. When the friction between particles A and B reaches a sufficient value, particle A will stick to particle B at the contact position.

Under this critical condition, the force balance for the depositing particle, A, can be given as

$$(F_g + F_n)\cos\beta_c + F_t \sin\beta_c = f_c[F_i + (F_g + F_n)\sin\beta_c + F_t\cos\beta_c], \quad (1)$$

where f_c is the static friction coefficient between particles. The lefthand side of Eq. 1 is the tangential force exerted on particle A, while the righthand side is the friction force. Each term in Eq. 1 will be analyzed prior to solving for β_c.

Net Drag Normal to the Filter Medium. Since the Reynolds number of flow in the laminar sublayer above the septum is always very small, the equations of motion and their boundary conditions both can be seen to be linear; therefore, the drag exerted on the particles can be solved for by using the reflection method, in which the velocity field is decomposed into a sum of subfields (Happel and Brenner, 1965). The behavior of the formed cake is treated as a porous medium except for the specific particles (such as particles A and B) to simplify the system. Thus, the flow field normal to the filter medium can be shown as in Figure 3a. In such a system, only the conditions of the two particles and the porous medium need to be considered, and the drag exerted on particle A normal to the filter medium is therefore given by

$$F_n = 6\pi\mu a(u_A - u_{B0A} - u^c_{A0A} - u^c_{B0A}), \quad (2)$$

where a is the radius of particle A, u_A is the relative velocity of particle A with respect to fluid flow, and u_{B0A} is the velocity field produced by reflection for the zeroth time from particle B and evaluated at particle A. The superscript c represents the reflected velocities due to the existence of the porous medium. From the analysis of Lu and Hwang (1993) for a similar system, the drag exerted on particle A can be expressed as

$$\frac{F_n}{6\pi\mu a u_A} = \cos\beta\,\mathbf{i}\left\{1 - \frac{3b}{2(a+b)}\left[1 - \left(\frac{2}{3}R_m b\right)^{0.5}\right] + \frac{9}{8}\left(\frac{a}{b + [(a+b)\cos\beta - a]}\right)\right\} + \sin\beta\,\mathbf{k}\left\{1 - \frac{3b}{4(a+b)}\left[1 - \left(\frac{2}{3}R_m b\right)^{0.5}\right] + \frac{9}{8}\left(\frac{a}{b + [(a+b)\cos\beta - a]}\right)\right\}, \quad (3)$$

where b is the radius of particle B, R_m is the filtration resistance of the porous medium, and $\mathbf{i}$ and $\mathbf{k}$ are the unit vectors, the directions of which are parallel and vertical to the line connected with the center of particles, respectively. The R_m term appears in the preceding equation due to the existence of the porous medium, which is quite different to the particles in an infinite flow field (Goren, 1979). In such a system, the net velocity of particle A, with respect to fluid flow, u_A, can be given as

$$u_A = q - v_l, \quad (4)$$

where q is the superficial velocity of the permeating fluid while v_l is the lift velocity of particle due to the inertial effect of tangential slurry flow. Vasseur and Cox (1976) have analyzed the lift force exerted on a neutrally buoyant spherical particle in two-dimensional shear flow. According to their results, v_l can be expressed as

$$v_l = \frac{1}{576}\frac{a^3}{\nu}\left(\frac{u_m^2}{\delta}\right)(1 - 2\kappa)(61 - 368\kappa), \quad (5)$$

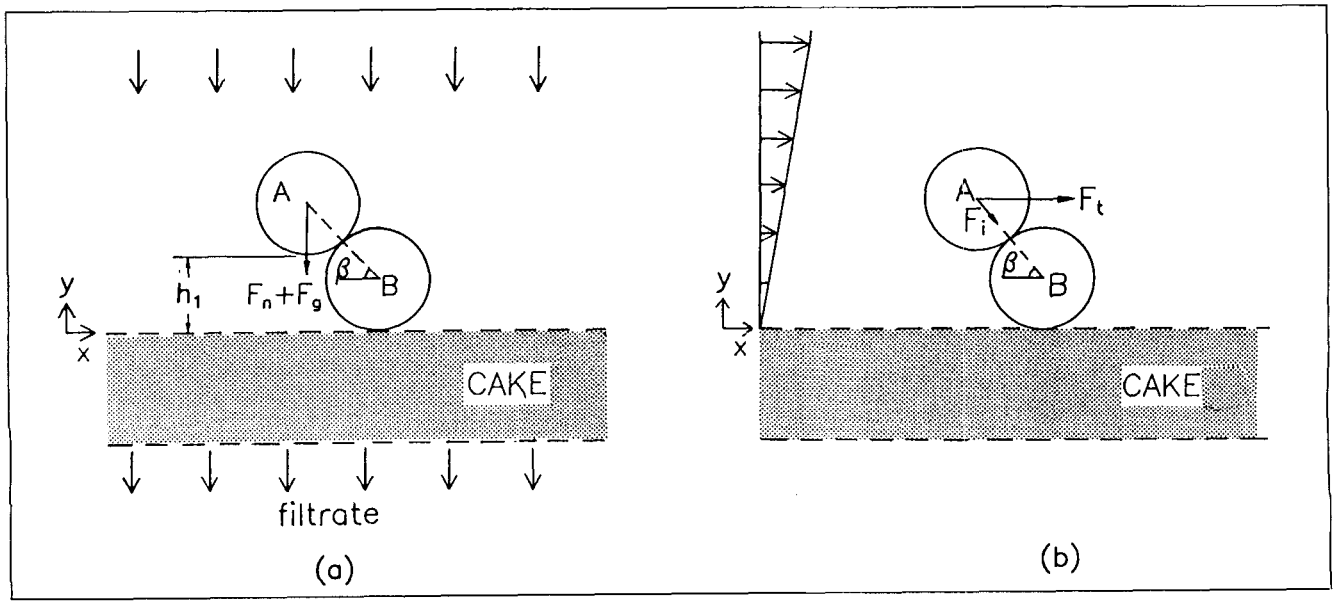

Figure 3. (a) Vertical flow around the depositing particle; (b) parallel flow around the depositing particle.

where δ is the thickness of the laminar sublayer, u_m is the tangential fluid velocity at the interface between the laminar sublayer and turbulent core, ν is the kinematic viscosity of the pure fluid, and κ is the ratio of the distance between particle A and porous medium to δ, that is, $\kappa = h_1/\delta$. For a fluid flowing turbulently in the two-parallel-plate cross-flow filtration filter,

$$\delta = \frac{5\nu}{u^*} = \frac{5\nu}{u_s\sqrt{f/2}}, \tag{6}$$

where u^* is the friction velocity, u_s is the average tangential velocity of fluid, and f is the Fanning friction factor. The experimental data of Belfort (1988) show that the value of f is higher for a flow in a porous tube than for a Poiseuille flow in a nonporous tube. Since in a filtration system the roughness of the cake surface varies with time as well as with the size of particles of the formed cake, it is quite difficult to have a simple expression to demonstrate this effect, so the value of f is estimated by the value of turbulent flow within a two-parallel-plate system, $f = 0.079\ Re^{-1/4}$, in this study for the sake of simplicity. Since the distance between particle A and the septum can be written as

$$h_1 = b + [(a+b)\sin\beta - a],$$

and κ is given by

$$\kappa = \frac{u_s h_1\sqrt{f/2}}{5\nu}, \tag{7}$$

it follows that F_n can be calculated by Eq. 3 if the operating conditions are known.

Tangential Drag Parallel to the Filter Medium. If the pore openings of the filtration septum correspond to a very small fraction of the septum area, the nonslip tangential flow can be assumed. Therefore, the flow field of fluid parallel to the filter medium can be simplified as in Figure 3b. In this flow field, the drag exerted on particle A can be expressed as

$$F_t = 6\pi\mu a(v_A - v_{B0A} - v^c_{A0A} - v^c_{B0A}), \tag{8}$$

where v represents the velocity subfield in the direction that is parallel to the filter medium, and the superscripts and subscripts in the equation are defined as in Eq. 2.

The undisturbed velocities of fluid at the gravity center of particles can be expressed as

$$v_A = \left(\frac{fu_s^2}{2\nu}\right)[b + (a+b)\sin\beta], \tag{9a}$$

$$v_B = \left(\frac{fu_s^2}{2\nu}\right)b. \tag{9b}$$

Following the analysis of Lu and Hwang (1993), the reflected velocity from particle B on particle A, v_{B0A}, can be given as

$$v_{B0A} = v_B\left(\frac{b}{a+b}\right)\left[\frac{3}{2}\cos\beta\,\mathbf{i} + \frac{3}{4}\sin\beta\,\mathbf{k}\right]. \tag{10}$$

Goldman et al. (1967) have used the reflection method to analyze the forces and torques exerted on a stagnant particle that stays in a simple shear flow field near a flat plane. Their results can be extended to calculate v^c_{A0A} as

$$v^c_{A0A} = -v_A\frac{9}{16}\frac{a}{b + (a+b)\sin\beta}. \tag{11}$$

For the flow field as shown in Figure 3b, O'Neill (1968) indicated that the corrected factor for Stokes' law due to the existence of a filter wall should be 1.7009; therefore,

$$v^c_{B0A} = -1.7009 v_{B0A}. \tag{12}$$

Substituting Eqs. 9–12 into Eq. 8, F_t can be given as

$$\begin{aligned} F_t = {} & 6\pi\mu a\left(\frac{fu_s^2}{2\nu}\right)[b + (a+b)\sin\beta] \\ & \times\left\{\mathbf{i}\cos\beta\left[1 + \frac{3b}{2(a+b)}\left(\frac{0.7009b}{b + (a+b)\sin\beta}\right)\right.\right. \\ & \left. + \frac{9}{16}\frac{a}{b + (a+b)\sin\beta}\right] \\ & + \mathbf{k}\sin\beta\left[1 - \frac{3b}{4(a+b)}\left(\frac{0.7009b}{b + (a+b)\sin\beta}\right)\right. \\ & \left.\left. + \frac{9}{16}\frac{a}{b + (a+b)\sin\beta}\right]\right\} \end{aligned} \tag{13}$$

Net Gravity Force of the Particle. The net gravity force of a spherical particle can be expressed as

$$F_g = \frac{\pi}{6}(\rho_s - \rho)gd_p^3. \tag{14}$$

Interparticle Force and Friction Factor between Particles. Applying the concept of the selective deposition of particles in a cross-flow filter (Lu and Ju, 1989), the net interparticle force and the friction factor between particles can be determined by conducting a cross-flow experiment for the given slurry (Lu and Hwang, 1993). According to this method, a series of experiments can be carried out to obtain the values of interparticle forces and friction factor for a given size of particles.

Once all of these forces and the friction coefficient between particles have been obtained under various conditions, the critical angle of friction, β_c, for each size of particles in slurry can be estimated by solving Eq. 1. Then, the calculated value of β_c can be used to determine whether the depositing particles are stable.

Forces exerted on the particles within a cake

During filtration, the filter cake is compressed continuously by the solid compressive pressure due to the friction drag of the liquid. The forces exerted on the deposited particles within a cake are analyzed to understand the course of

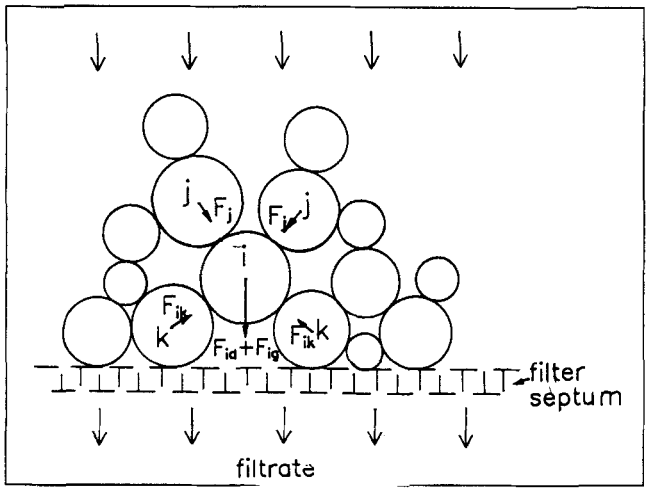

Figure 4. Forces exerted on the deposited particles.

compression of the cake. Then, the variation of cake properties can be simulated and is discussed in the next section.

In this study, flow of filtrate within the cake is assumed to be one-dimensional flow; therefore, tangential shear force due to cross-flow of slurry is assumed to be only acting on the surface of the cake. The frictional drag exerted on the spherical particles within a cake can be estimated by the result of Happel and Brenner (1965) as

$$F_d = -4\pi\mu \frac{av(3+2\gamma^5)}{2-3\gamma+3\gamma^5-2\gamma^6} \tag{15}$$

where $\gamma = \sqrt[3]{(1-\epsilon)}$. Thus, the drag exerted on the particles within a cake can be used to estimate when the local velocity of filtrate, v, and the local porosity of cake, ϵ, are known.

Figure 4 shows a sketch of particle packing in a filter cake. Since the forces exerted on the upper particles would be transmitted to the surrounded particles through the contact points, the forces exerted on particle i can be expressed as

$$F^i = \sum_j \left[\left(F^j \cdot n_{ji}\right) n_{ji}\right] + \sum_k F_{ik} + F_{id} + F_{ig}, \tag{16}$$

where j represents all of the surrounding particles, which are located above particle i, while the k particles are located beneath particle i. The total forces, F^i and F^j, are exerted on particles i and j, respectively; n_{ji} is the unit vector of the direction that is parallel to the line connected with the center of particles i and j; F_{ik} is the interparticle force between particles i and k; F_{id} is the drag exerted on particle i, which can be estimated from Eq. 15; and F_{ig} is the net gravity force on particle i. Prior to calculating the total forces exerted on particle i by using Eq. 16, the forces exerted on all of the surrounding particles located above particle i should be calculated. Therefore, the force analysis of particles is carried out from the cake surface toward the filter septum, and the details of the analysis are given in the following section.

Simulation of cake formation during a cross-flow filtration

Two-dimensional (2-D) cake formation is quite different from the 3-D version due to the resulting configurations; however, 2-D simulation results can provide some help in understanding the characteristics of the cross-flow filtration system. Based on the preceding force analysis, a numerical program was designed to simulate the particle deposition and migration within the formed cake during cross-flow filtration. The 2-D structure of the formed cake can be simulated under various operating conditions, which can provide the particle-size distribution of cake and the variations of local cake properties. The flow chart of the simulation program is shown in Figure 5, and the procedures are described as follows.

Particle Generation. If the operating variables, such as the tangential velocity of slurry, filtration rate, and channel clearance, are known, the numerical method proposed by Lu et al. (1993) can be used to calculate the instantaneous flux of particles that are transported and arrive at the cake surface, N_b. Since the ratio of the eddy diffusivity of particles to the eddy viscosity of fluid in our study is very close to 1 (Lu et al., 1993), the particles that arrive at the cake surface have almost the same size distribution as that of the initial slurry.

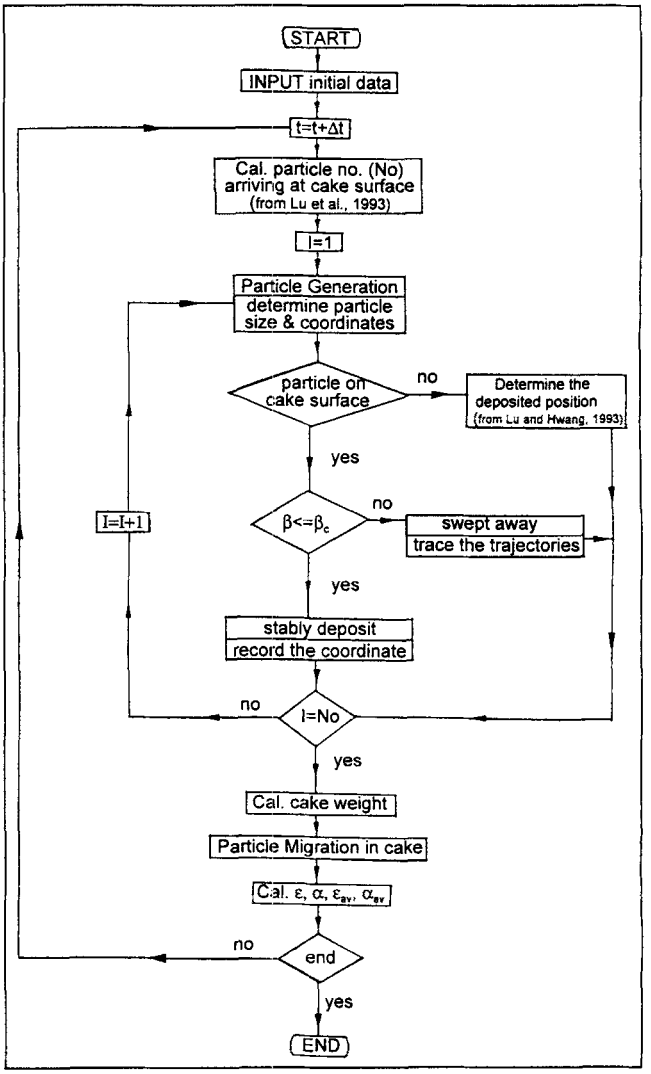

Figure 5. Simulation of cake formation in cross-flow filtration.

Thus, the number of particles instantaneously arriving at the cake surface, N_0, can be calculated accordingly if the density and the size distribution of particles are known. In the simulation process, the instantaneous number of generated particles is the same as N_0. The size of particles that arrive at the cake surface is determined in accord with an exponential-type random function, which may be available from the size measurement of the used particulate sample, while the initial locations of particles transported to the laminar sublayer by turbulent eddies are determined by a generator with a random distribution function.

Particle Deposition on the Cake Surface. As soon as the slurry particle arrives at the cake surface and touches the particle deposited on the cake surface, the friction angle between the deposited particles, β, is estimated to examine its stability. If $\beta \le \beta_c$, the particle will stably deposit at the point where it touches the cake surface; otherwise, it will be swept away from its contact point and may settle at another stable position downstream or be reentrained in the bulk flow of slurry. The strength of forces exerted on each deposited particle and its deposited location are recorded for further calculation during the simulation.

If a depositing particle is carried by filtrate and migrates into the pores of the cake, the deposited place of the particle will be determined by the simulation process in the same way as in dead-end cake filtration because of the assumption of one-dimensional flow in the cake, which is described in our previous article (Lu and Hwang, 1993).

The local cake porosity is estimated after each time increment. The ratio of the wet-to-dry mass of the cake on the cake surface is obtained accordingly.

Mass of the Formed Cake. As the value of N_b is calculated, the mass flux of particle deposition can be given by

$$N_w = \int_0^\infty N_b f_0(d_p) P(d_p)\, dd_p, \tag{17}$$

where $f_0(d_p)$ is the frequency distribution function of particle size in slurry, while $P(d_p)$ is the probability function of particle deposition. For any specific particle on the cake surface, for example, particle B in Figure 1, $P(d_p)$ can be seen to be the ratio of the area on which slurry particles can stably deposit to the total area in which particles can touch the particle, that is,

$$P(d_p) = \frac{\beta_c}{\pi/2}. \tag{18}$$

The probability of particle deposition of each size is calculated from Eq. 18 in order to obtain N_w during the simulation. The mass of formed cake is therefore given by

$$w_i = N_w \Delta t, \tag{19}$$

where Δt is the incremental time.

Velocity of Filtrate Flow within the Cake. From the analysis of mass balance, the generalized expression of q_i/q_1 for a variable pressure filtration is (Lu and Tiller, 1969)

$$\frac{q_i}{q_1} = \frac{[(1-s)(1-\epsilon_{av} - L(d\epsilon_{av}/dL)) - (m_i - 1)(1-\epsilon_i)s](1-\epsilon_{av})}{[(1-ms)(1-\epsilon_{av} - L(d\epsilon_{av}/dL))(1-\epsilon_{av}) - sL(d\epsilon_{av}/dL)\rho/\rho_s]}. \tag{20}$$

For a constant pressure filtration, the ratio of q_i to q_1 can be reduced to (Tiller and Cooper, 1960)

$$\frac{q_i}{q_1} = \frac{1-m_i s}{1-ms} + \frac{\epsilon_i - \epsilon_{av}}{1-\epsilon_{av}} \frac{m_i - 1}{1-ms} s. \tag{21}$$

The rate of filtration, q_1, can be evaluated from the mass of filtrate; then, the value of q_i can be calculated from Eqs. 20 or 21.

Since the local fluid velocity of filtrate within a cake can be given by

$$\left.\frac{dq}{dx}\right|_t = \left.\frac{d\epsilon}{dt}\right|_x,$$

or in a difference form,

$$q_{x+\Delta x,t} = q_{x,t} - \frac{\Delta x}{\Delta t}(\epsilon_{x,t-\Delta t} - \epsilon_{x,t}), \tag{22}$$

the values of local porosity, ϵ_x, which are obtained in the previous and present time interval are used to estimate local fluid velocity by Eq. 22.

Migration of Unstable Particles in Cake. The net force exerted on each particle within a cake can be calculated by using Eq. 16. For each contact point of a specific particle with a nearby particle, the net force exerted on the particle can be divided into two vectors, the directions of which are parallel and vertical to the line drawn through the centers of gravity of the two particles and the contact point, respectively. If the frictional force is not large enough to enable the particle to stick, the particle will roll off the contact point and move to the other location. The velocities and the displacements of separating particles can be determined by integrating Newton's second law of motion.

Local Cake Porosity. After each time increment, the filter cake is divided into several layers to estimate its local porosity. For particles with irregular shape, the simulated packing porosity of spherical particles can be corrected by introducing the shape factor of particles, and the value of its local porosity can be estimated according to Lu and Hwang (1993):

$$\epsilon = 1 - (1 - \epsilon_{sph})\phi_s \qquad \text{for} \quad \phi_s \ge 0.7, \tag{23}$$

where ϵ_{sph} is the porosity of the spherical particulate bed with the same hydrodynamic size distribution.

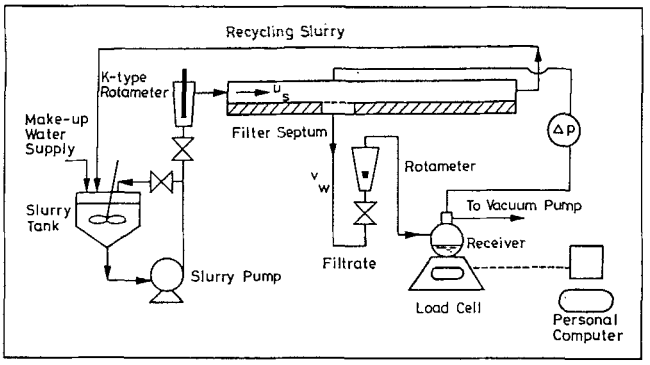

Figure 6. Experimental cross-flow filtration system.

Local Specific Filtration Resistance. Comparing the Kozeny equation with the differential form of the equation of filtration, the specific filtration resistance of a cake can be related to the porosity of the formed cake as

$$\alpha = kS_0^2 \frac{(1-\epsilon)}{\epsilon^3 \rho_s}, \tag{24}$$

where S_0 is the specific surface area of particles, which can be obtained from various experimental measurements. Since the Kozeny constant in Eq. 24 is given as (Happel and Brenner, 1965)

$$k = \frac{2\epsilon^3}{(1-\epsilon)[\ln\{1/(1-\epsilon)\} - \{1-(1-\epsilon)^2\}/\{1+(1-\epsilon)^2\}]}, \tag{25}$$

and is a function of ϵ, the value of k should be calculated in accord with the change in the value of local porosity during the simulation. Once the local porosity of the cake and the values of k, S_0, and ρ_s are known, the value of the corresponding local specific filtration resistance in the cake can be estimated from Eq. 24.

By repeating the steps just given, the variation of cake properties can be simulated for the entire path of a cross-flow filtration.

Experimental Studies

Cross-flow filtration experiments were carried out in the 2-D cross-flow filtration system shown in Figure 6. The details of construction of the filter can be found in the authors' previous article (Lu et al., 1993). A light $CaCO_3$ slurry of 0.25–0.5 wt% was prepared and filtered under various operating conditions. The shape factor of the $CaCO_3$ particles was 0.72, and their size distribution and shape are shown in Figures 7a and 7b, respectively. The weight of the received filtrate was determined by a load cell and was recorded by a personal computer during the experiment. The cake thickness was measured from the transparent acrylic upper plate of the filter by a vernier. As soon as the experiment was terminated, the filter cake that had formed on the filter medium was carefully scraped, the dry mass of the cake was determined, and the particle-size distribution was analyzed by a Microtrac optical size analyzer. The average porosity of the cake was then calculated from measurements of the dry mass and the thickness of cake.

Results and Discussions

Critical angle of friction on the cake surface

Once the interparticle force and the friction coefficient between particles have been measured, the critical angle of friction, β_c, for each particle size can be calculated by using Eq. 1. Figure 8 shows that the calculated values of β_c vary with the filtration rate for three different sizes of spherical particles. Since the attenuation of filtration rate will decrease the normal drag on particles staying on the cake surface, the value of β_c also decreases as q decreases. These results also indicate that the larger the particle is, the smaller the value of β_c will be. This fact implies that a smaller particle will deposit on the cake surface more stably than will a larger one.

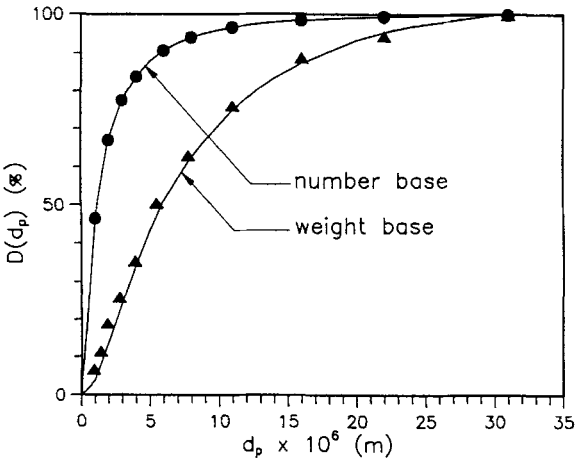

(a)

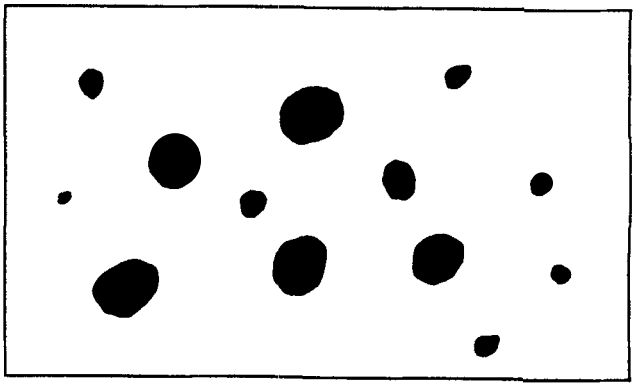

(b)

Figure 7. (a) Particle-size distribution of $CaCO_3$; (b) particle shape of $CaCO_3$.

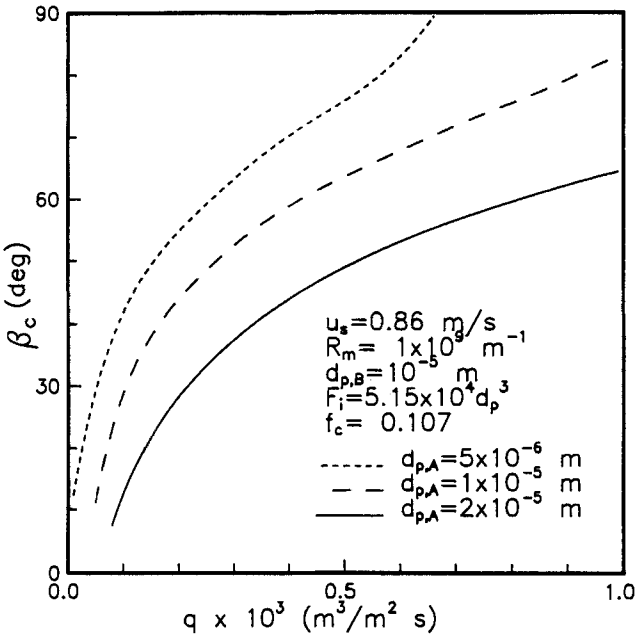

Figure 8. Effects of q and d_{pa} on β_c of particle A.

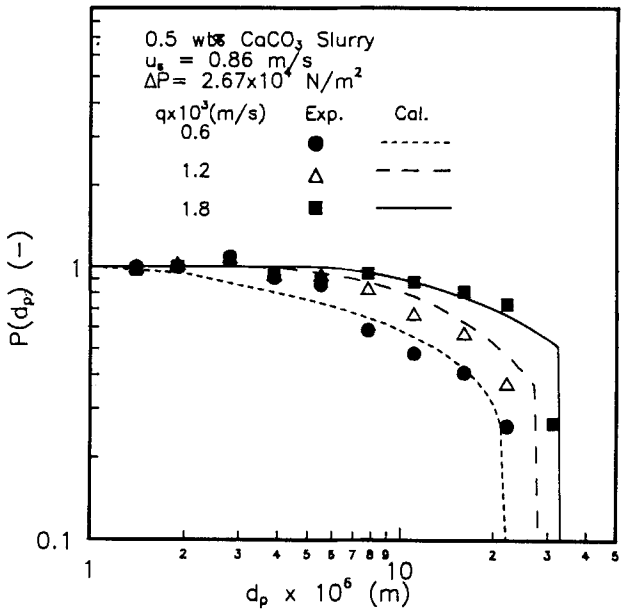

Figure 10. Probability of particle deposition on cake surface under various filtration rates in cross-flow filtration.

The effect of slurry velocity on the value of β_c is demonstrated in Figure 9. For a given size of d_p, a higher slurry velocity results in a smaller β_c, which will make it more difficult for particles to deposit on the surface of septum to form cake.

Probability of particle deposition

Besides the fact that the probability of particle deposition can be estimated from Eq. 18, it also can be predicted from the equation derived from a particle balance for the slurry arriving at the cake surface, that is,

$$P(d_p) = \frac{f_c(d_p) N_w}{f_0(d_p) C_w q}, \tag{26}$$

where $f_c(d_p)$ is the frequency function of the size d_p in the formed cake. Each term on the righthand side of Eq. 26 can be obtained from experimental measurements, except the particle concentration at the cake surface, C_w, which can be estimated by using the numerical method given by Lu et al. (1993).

Figure 10 shows the plots of probability of particle deposition against particle diameter under three different filtration rates. The curves shown in the figure were calculated by using Eq. 18, while the points represent the experimental results that were estimated from Eq. 26. These results clearly demonstrate that there exists a critical cut-diameter, d_{pc}, for particle deposition under given conditions (Lu and Ju, 1989). As a result, particles with diameters smaller than d_{pc} will deposit on the septum, and the probability of particle deposition suddenly reduces to a negligible value when d_p exceeds the value of d_{pc}. This result confirms the existence of the selective cut-diameter in a cross-flow filtration (Lu and Ju, 1989).

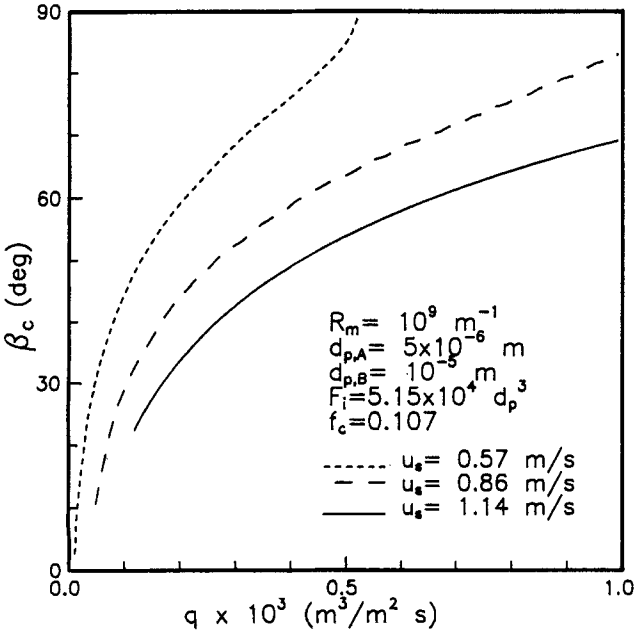

Figure 9. Effects of q and u_s on β_c of particle A.

Particle-size distribution in a cake

In Figure 11, the variation of the particle-size distribution in the cake at $x = 0.05$ m during a cross-flow filtration is shown. At each setting for filtration time, the experiment was terminated, and the cake thickness and the particle-size distributions in the cake surface layer were measured. The theo-

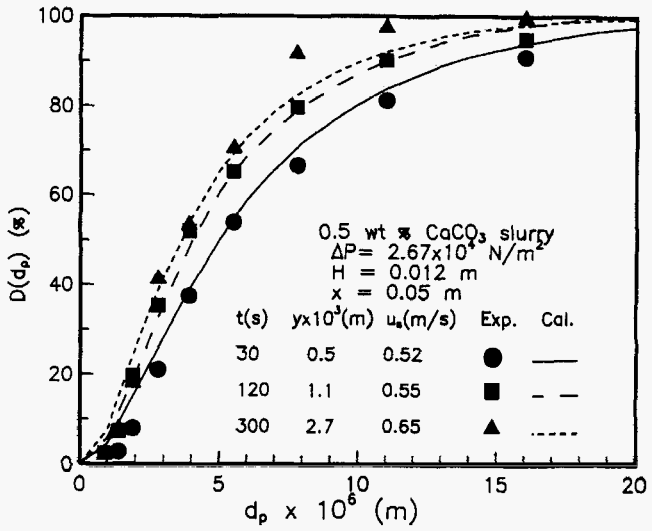

Figure 11. Variation of particle-size distribution in cake surface in a cross-flow filtration.

retical size distribution of particles shown in the figure can be calculated as follows: The cross-sectional area and the velocity of slurry flow were corrected from the measured cake thickness. Based on the known conditions, the value of β_c can be calculated from Eq. 1 and can be substituted into Eq. 18 to calculate $P(d_p)$. Then, the amount of deposition for each particle size and the theoretical values of $D(d_p)$ can be estimated. Figure 11 shows that an upper layer of the cake (larger y) has a smaller size distribution of particles. This is due to the decay of filtration rate during filtration. The figure also shows good agreement between the calculated results and the experimental data except for the case of $t = 300$ s. This result is probably due to an unclear critical cut-diameter for the case of smaller q at larger t (see Figure 10).

Packing structure of particles

Figures 12a–12c show the simulated packing structures of spherical particles (using the properties of $CaCO_3$) on the cake surface under various conditions. The configurations and the size distributions of the deposited particles in the figure are quite different from the similar simulated results obtained in dead-end cake filtration shown in Figure 12d (Lu and Hwang, 1993) due to the existence of tangential flow. These figures show that the particles deposited in the forming cake at the initial stage in cross-flow filtration are packed with an angle with respect to the direction of filtration, and also show that the particle-size distribution of the cake in cross-flow filtration is always smaller than that in cake filtration. The effect of the tangential velocity of slurry on the cake structure can be seen from the comparison of Figures 12a and 12b. The larger the tangential velocity is, the smaller the cut-diameter; thus, in Figure 12b more small particles can be observed in the cake structure. By comparing the cake structures shown in Figures 12a and 12c, one can see how the rate of filtration also affects the cake structure; the smaller filtration rate clearly reduces the size of cut-diameter, and results in finer particles in the composition.

From the simulated results, the effect of tangential velocity on the cake surface porosity is shown in Figure 13. Since the packing of particles in a cake is a random process, the simulated results have scattered values under given conditions. Regressive analysis, however, shows that the porosity on the cake surface increases gradually with the increase of tangential velocity. Figure 14 is a plot of simulated values of ϵ_i against filtration rate. It can be seen that a smaller q will result in a higher value of ϵ_i since a smaller normal drag is exerted on the particles.

Figures 15a–15c depict how the formed cake is compressed as filtration time passes by. Figure 15a is the packing structure of particles at the initial stage and is similar to Figure 12. From the movement of the numbered particles in enlarged Figures 15a and 15b, one can see that the unstable particles in the original structure move toward the septum due to the drag forces, which results in a more compacted cake. The increase of fine particles near the septum with time in these enlarged pictures clearly shows that more fines will migrate toward the septum and construct a higher resistance cake. These simulation results demonstrate the fact that the attenuation of filtration rate in a cross-flow filtration is not only due to compression of the cake but also the fine migration within the cake.

Distribution of porosity in a growing cake

In Figure 16, the simulated porosity distributions of a growing cake formed at $x = 0.15$ m under the condition of $u_s = 1.0$ m/s and $\Delta P = 2.67 \times 10^4$ N/m^2 are shown. From the curves shown in Figure 16, one can see that the filter cake is continuously compressed by frictional drag, which causes the local cake porosity to decrease gradually. These curves also clearly show that, in constant pressure filtration, the cake is compressed at a very early stage of filtration because the whole solid compressive pressure is exerted on the formed cake at the beginning of filtration; thus, the greatest variation of cake porosity is observed near the septum, and a flatter porosity distribution is seen near the surface. It is interesting to note that the porosity on the cake surface, ϵ_i, increases gradually as time increases, which is due to the fact that the attenuation of filtration rate during filtration results in a looser packing of particles (Figure 14).

Figure 17 shows the variations of average cake porosity at $x = 0.15$ m during cross-flow filtrations under two different cross-flow velocities. In the range of our experiments, the figure shows that the effect of u_s on ϵ_{av} at a given x is nearly negligible. This may be due to the fact that the packing porosity of particles has almost the same value as u_s increases from 0.5 to 1.0 m/s (Figure 14). Since ϵ_i increases gradually during filtration (Figure 14), it can be found that ϵ_{av} increases, too. In general, the simulated results agree fairly well with the experimental data for most periods of filtration; however, a larger deviation is found between the simulated values and the experimental data at the beginning of filtration for smaller values of u_s. This fact may be due to a slight underestimation of N_w under the condition of small u_s by using the theory of Lu et al. (1993), which leads to a smaller N_0, and results in a higher calculated porosity of the formed cake.

Figure 18 shows the profile of ϵ_{av} of the formed cake in

the x direction at $t = 1{,}000$ s under the condition of $u_s = 1.0$ m/s and $\Delta P = 2.67 \times 10^4$ N/m^2. Since both the tangential velocity of the slurry and the filtration pressure drop decrease gradually along the x direction, the values of ϵ_{av} are almost the same along the x direction due to these two contradictory effects. The good agreement between the experimental data and the simulated results shown in the figure demonstrates that the simulation process can be used to predict cake formation in cross-flow filtrations.

Distribution of specific filtration resistance in a filter cake

Figure 19 shows the simulated profiles of local α vs. cake thickness at $x = 0.15$ m. The value of local α shows the high-

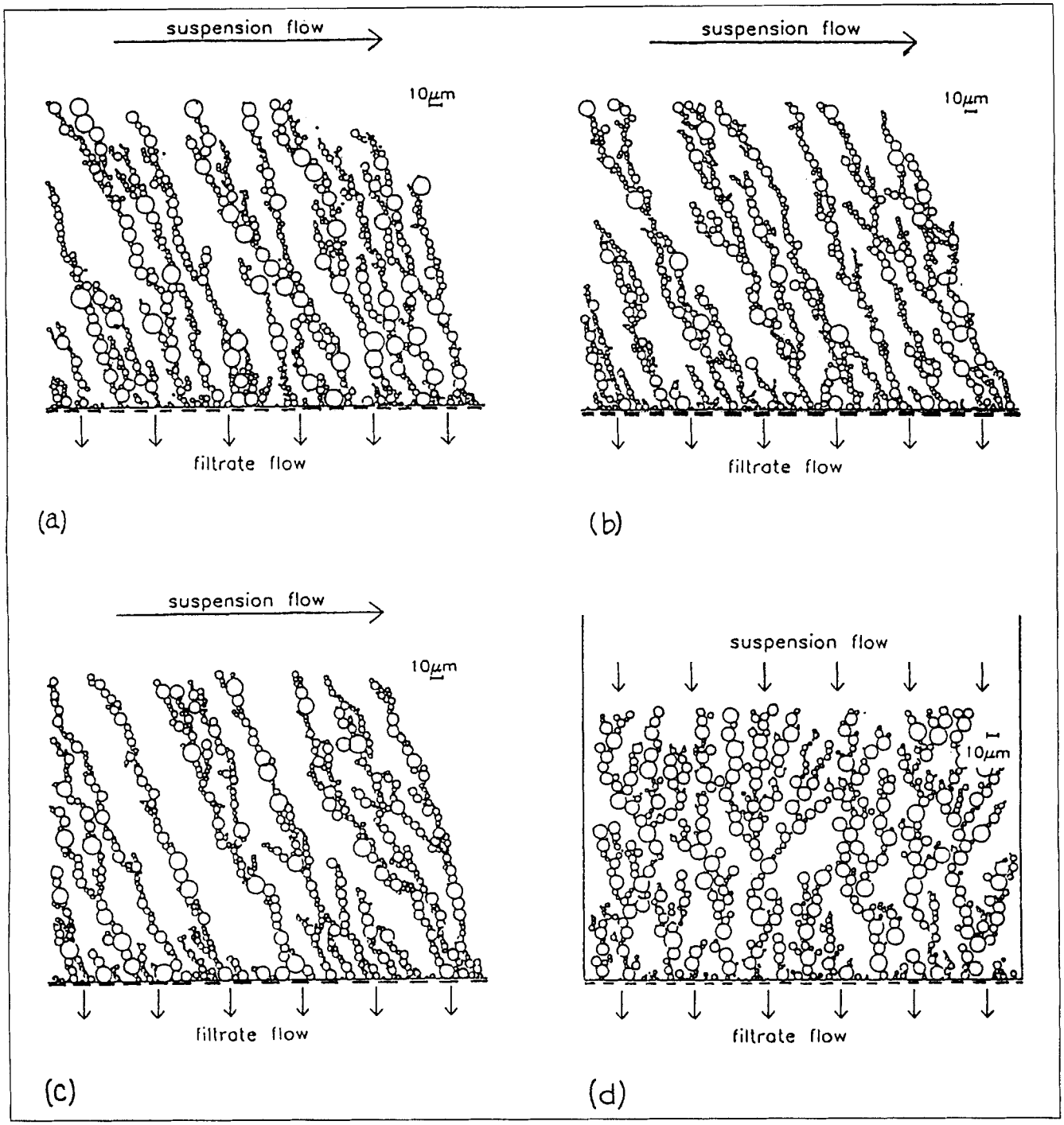

Figure 12. Packing structure of particles on cake surface under various operating conditions.

(a) $u_S = 0.86$ m/s, $q = 0.001$ m^3/m^{2}s, $\Delta P = 26{,}656$ N/m^2. (b) $u_S = 1.72$ m/s, $q = 0.001$ m^3/m^{2}s, $\Delta P = 26{,}656$ N/m^2. (c) $u_s = 0.86$ m/s, $q = 0.0002$ m^3/m^{2}s, $\Delta P = 26{,}656$ N/m^2. (d) "Dead-end" cake filtration.

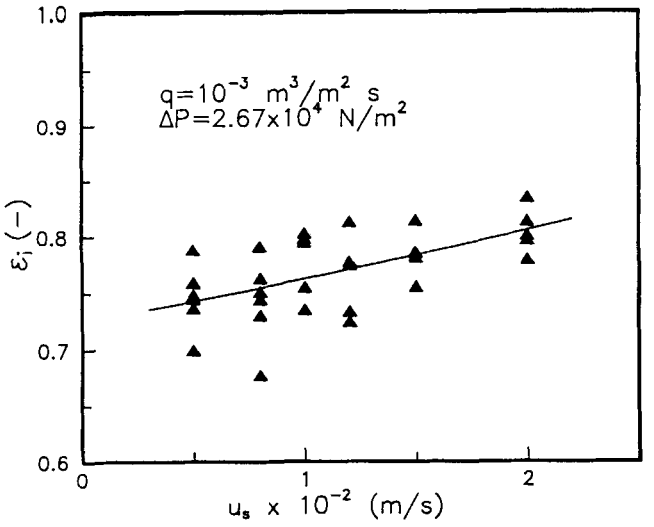

Figure 13. Effect of u_s on ϵ_i.

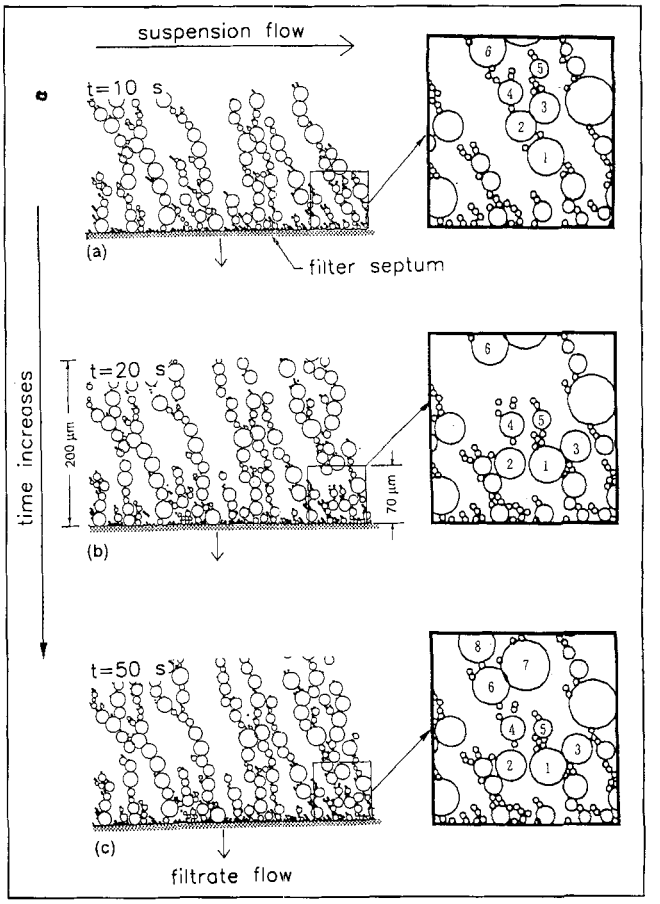

Figure 15. Packing structure of particles in cake.

(Operating condition: $u_s = 1.0$ m/s, $\Delta P = 2.67 \times 10^4$ N/m^2, $x = 0.15$ m.) (a) $t = 10$ s; (b) $t = 20$ s; (c) $t = 50$ s.

est resistance at the surface of the filter septum and decreases abruptly in the y direction. For the cases with filtration time greater than 500 s, the curve of local α vs. y shows an up and down profile, which is quite different from a monotonic one as seen in dead-end filtration (Lu and Hwang, 1993), and the value of α at the cake surface may not be the lowest value. The value of α is not only affected by the value of the effective specific surface area, S_0, of the cake materials, but is also affected by the value of the porosity of the formed cake. During cross-flow filtrations, the decrease in q causes the decrease in the diameters of the deposited particles and also results in an increase in cake porosity; on the other hand, the decrease in the value of the tangential velocity will also cause a decrease in porosity. Thus, the value of local α varies up and down near the cake surface with these opposing effects.

In Figure 20 the variations of α_{av} with time at $x = 0.15$ m for two different cross-flow velocities are shown. Since the high slurry velocity leads to finer particles in the formed cake, the case of $u_s = 1.0$ m/s shows a higher value of α_{av} than

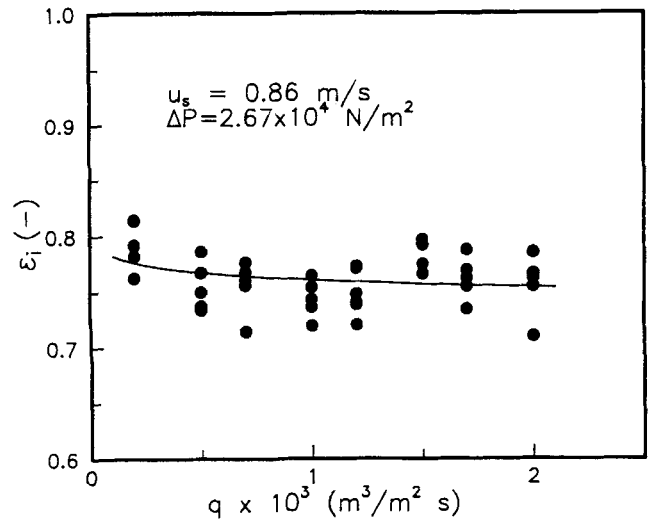

Figure 14. Effect of q on ϵ_i.

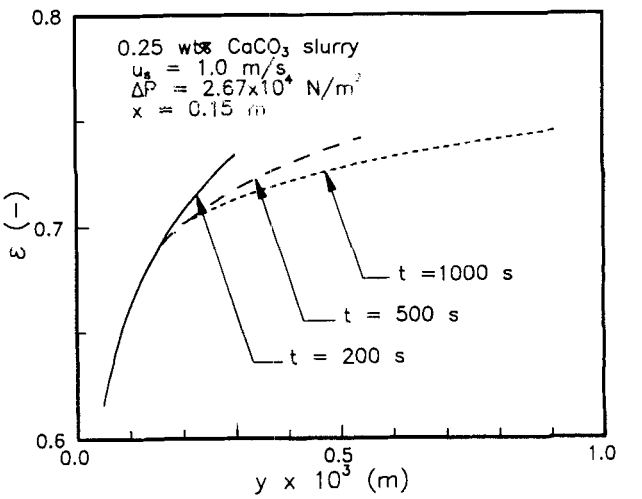

Figure 16. Variation of ϵ profile in cake during a cross-flow filtration at $u_s = 1$ m/s.

does the case $u_s = 0.5$ m/s. The experimental result of $u_s = 0.5$ m/s shown in the figure illustrates that the value of α_{av} decreases at the beginning of filtration and increases gradually as t exceeds 1,000 s. This down and up variation may be due to the increase of ϵ_{av} at the beginning of filtration as described in Figure 17 and the increase of finer particles later as described in Figure 11. The simulated result for the case, however, shows a monotonous decrease in α_{av} vs. time (see Figure 11). Comparing the simulated results and the experimental data, excellent agreement is observed for the case of $u_s = 1.0$ m/s, while quite a large deviation is found for the case of $u_s = 0.5$ m/s. The cause of this deviation is the underestimation of N_w as described in the discussion of Figure 17.

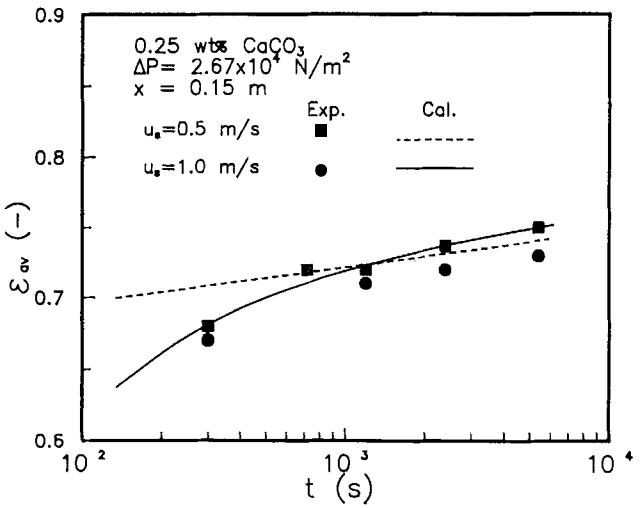

Figure 17. Variation of ϵ_{av} with time under different u_s during cross-flow filtrations.

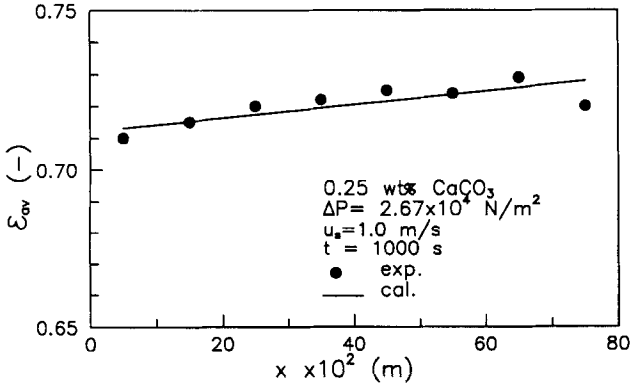

Figure 18. Profile of ϵ_{av} in the x direction.

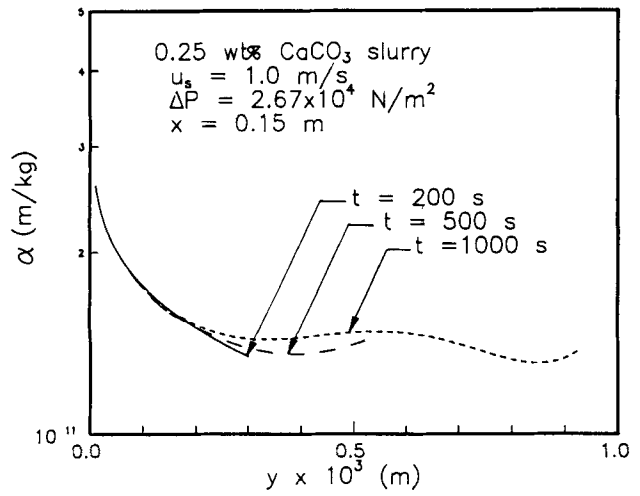

Figure 19. Variation of α profile in cake during a cross-flow filtration at $u_s = 1$ m/s.

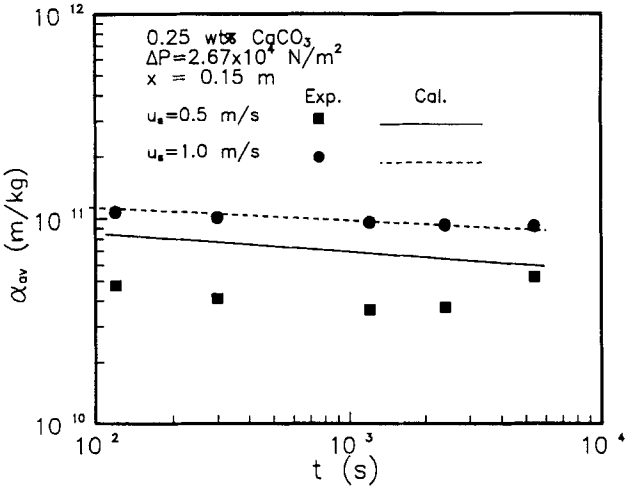

Figure 20. Variation of α_{av} with time under different u_s during cross-flow filtrations.

Figure 21 shows the profile of α_{av} of the formed cake in the x direction under the same conditions as shown in Figure 18. Since the size distribution of particles will increase along the x direction due to the decrease of the tangential velocity of the slurry, the value of α_{av} decreases slightly along the x direction for a given filtration time. Good agreement can also be seen between the experimental data and the simulated results in the figure.

Conclusion

The forces exerted on depositing particles have been analyzed and the values of critical friction angle calculated for given conditions. The probability of particle deposition and

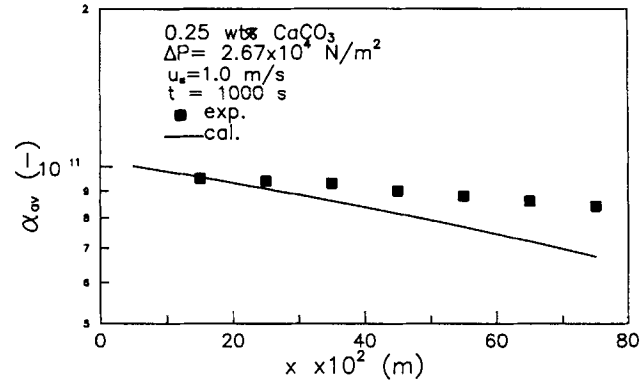

Figure 21. A profile of α_{av} in the x direction.

the particle-size distribution in a cake have been exactly estimated from the value of β_c. A numerical program has been established to simulate not only the packing structure of particles, but also the variations of the local cake properties during a cross-flow filtration. The effects of cross-flow velocity and filtration rate on cake formation have been discussed in detail. The calculated average cake porosity and average filtration resistance agreed fairly well with the experimental data.

Acknowledgment

The authors wish to express their sincere gratitude to the National Science Council of the Republic of China for its financial support.

Notation

h_1 = distance between particle A and porous medium, m
L = cake thickness, m
m = weight ratio of wet to dry cake
ΔP = total pressure drop of filtration, N/m^2
P_i = pressure below which porosity is constant, N/m^2
P_s = local solid compressive pressure, N/m^2
s = concentration of slurry
u_s = average cross-flow velocity of slurry, m/s
x = coordinate which direction parallel to the tangential flow of slurry
y = coordinate which direction parallel to the growth of cake

Greek letters

α = specific filtration resistance, m/kg
μ = viscosity of fluid, kg/s·m
ρ = density, kg/m^3

Subscripts

i = properties at the surface of filter cake
j = properties in the jth layer of filter cake
s = solid
w = property at septum surface

Literature Cited

Altena, F. W., and G. Belfort, "Lateral Migration of Spherical Particles in Porous Flow Channels: Application to Membrane Filtration," *Chem. Eng. Sci.*, **39**(2), 343 (1984).

Belfort, G., "Membrane Modules: Comparison of Different Configurations Using Fluid Mechanics," *J. Memb. Sci.*, **35**, 245 (1988).

Belfort, G., "Fluid Mechanics in Membrane Filtration: Recent Developments," *J. Memb. Sci.*, **40**, 123 (1989).

Davis, R. H., and D. T. Leighton, "Shear-induced Transport of a Particle Layer along a Porous Wall," *Chem. Eng. Sci.*, **42**(2), 275 (1987).

Fischer, E., and J. Raasch, "Cross-flow Filtration," *Ger. Chem. Eng.*, **8**, 211 (1986).

Goldman, A. J., R. G. Cox, and H. Brenner, "Slow Viscous Motion of a Sphere Parallel to a Plane Wall: II. Couette Flow," *Chem. Eng. Sci.*, **22**, 653 (1967).

Goren, S. L., "The Hydrodynamic Force Resisting the Approach of a Sphere to a Plane Permeable Wall," *J. Colloid Interf. Sci.*, **69**, 78 (1979).

Green, G., and G. Belfort, "Fouling of Ultrafiltration Membranes: Lateral Migration and the Particle Trajectory Model," *Desalination*, **35**, 129 (1980).

Happel, J., and H. Brenner, *Low Reynolds Number Hydrodynamics*, Chaps. 6–8, Prentice-Hall, Englewood Cliffs, NJ (1965).

Houi, D., and R. Lenormand, "Particle Accumulation at the Surface of a Filter," *Filtr. Sep.*, 238 (1986).

Kleinstreuer, C., and T. P. Chin, "Analysis of Multiple Particle Trajectories and Deposition Layer Growth in Porous Conduits," *Chem. Eng. Commun.*, **28**, 193 (1984).

Lu, W. M., and F. M. Tiller, "A Modified Definition of Average Specific Filtration Resistance for a Variable Pressure Filtration," *Bull. College Eng., Nat. Taiwan Univ.*, **13**, 77 (1969).

Lu, W. M., and S. C. Ju, "Selective Particle Deposition in Cross-flow Filtration," *Sep. Sci. Technol.*, **24**(7,8), 517 (1989).

Lu, W. M., K. J. Hwang, and S. C. Ju, "Studies on the Mechanism of Cross-flow Filtration," *Chem. Eng. Sci.*, **48**, 863 (1993).

Lu, W. M., and K. J. Hwang, "Mechanism of Cake Formation in Constant Pressure Filtrations," *Sep. Technol.*, **3**, 122 (1993).

Murkes, J., and G. G. Carlsson, *Crossflow Filtration*, Wiley, New York (1988).

O'Neill, M. E., "A Sphere in Contact with a Plane Wall in a Slow Linear Shear Flow," *Chem. Eng. Sci.*, **23**, 1293 (1968).

Porter, M. C., "Concentration Polarization with Membrane Ultrafiltration," *Ind. Eng. Chem. Prod. Res. Dev.*, **11**(3), 234 (1972).

Romero, C. A., and R. H. Davis, "Global Model of Crossflow Microfiltration Based on Hydrodynamic Particle Diffusion," *J. Memb. Sci.*, **39**, 157 (1988).

Romero, C. A., and R. H. Davis, "Transient Model of Crossflow Microfiltration," *Chem. Eng. Sci.*, **45**, 13 (1990).

Schmitz, P., C. Gouverneur, D. Houi, and M. Madianos, "Theoretical Model at Pore Scale for Particle Deposition on a Crossflow Microfiltration Membrane," *Proc. World Filtration Cong.*, Nice, France p. 571 (1990).

Sharma, M. M., and Z. Lei, "A Model for Clay Filter Cake Properties," *Colloids Surf.*, **56**, 357 (1991).

Tassopoulos, M., J. A. O'Brien, and D. E. Rosner, "Simulation of Microstructure/Mechanism Relationships in Particle Deposition," *AIChE J.*, **35**(6), 967 (1989).

Tiller, F. M., "The Role of Porosity in Filtration—Numerical Methods for Constant Rate and Constant Pressure Filtration Based on Kozeny's Law," *Chem. Eng. Prog.*, **49**(9), 467 (1953).

Tiller, F. M., and H. Cooper, "The Role of Porosity in Filtration: IV. Constant Pressure Filtration," *AIChE J.*, **6**(4), 595 (1960).

Vasseur, P., and R. G. Cox, "The Lateral Migration of Spherical Particle in Two Dimensional Shear Flow," *J. Fluid Mech.*, **78**, 385 (1976).

Zydney, A. L., and C. K. Colton, "A Concentration Polarization Model for the Filtrate Flux in Cross-Flow Microfiltration of Particulate Suspensions," *Chem. Eng. Commun.*, **47**, 1 (1986).

Manuscript received Nov. 30, 1993, and revision received June 6, 1994.